New Journal of Physics
The open access journal at the forefront of physics

Deutsche Physikalische Gesellschaft DPG IOP Institute of Physics

PAPER • OPEN ACCESS

# Dynamic ion shadows behind finite-sized objects in collisionless magnetized plasma flows

To cite this article: W J Miloch *et al* 2018 *New J. Phys.* **20** 073027

View the article online for updates and enhancements.

Related content

- Wake effects and Mach cones behind objects
Wojciech J Miloch
- Wake potential of a dust particle in magnetised plasmas
W J Miloch, D Darian and M Mortensen
- On the wake structure in streaming complex plasmas
Patrick Ludwig, Wojciech J Miloch, Hanno Kählert et al.

Recent citations

- Experiments on wake structures behind a microparticle in a magnetized plasma flow
Hendrik Jung *et al*

IOP ebooks™

Bringing you innovative digital publishing with leading voices to create your essential collection of books in STEM research.

Start exploring the collection - download the first chapter of every title for free.

This content was downloaded from IP address 129.240.84.21 on 27/08/2018 at 11:32

New Journal of Physics
The open access journal at the forefront of physics

Deutsche Physikalische Gesellschaft DPG
IOP Institute of Physics

Published in partnership with: Deutsche Physikalische Gesellschaft and the Institute of Physics

OPEN ACCESS

RECEIVED
9 May 2018

REVISED
21 June 2018

ACCEPTED FOR PUBLICATION
2 July 2018

PUBLISHED
17 July 2018

Original content from this work may be used under the terms of the Creative Commons Attribution 3.0 licence.

Any further distribution of this work must maintain attribution to the author(s) and the title of the work, journal citation and DOI.

PAPER

# Dynamic ion shadows behind finite-sized objects in collisionless magnetized plasma flows

**W J Miloch**[1], **H Jung**[2], **D Darian**[3], **F Greiner**[2], **M Mortensen**[3] and **A Piel**[2]

[1] Department of Physics, University of Oslo, PO Box 1048 Blindern, NO-0317 Oslo, Norway
[2] IEAP, Christian-Albrechts-Universität, D-24098 Kiel, Germany
[3] Department of Mathematics, University of Oslo, Postboks 1053 Blindern, NO-0316 Oslo, Norway

**E-mail:** w.j.miloch@fys.uio.no

**Keywords:** complex plasmas, wake formation, dust charging, dusty plasma, magnetized plasma flow

## Abstract

The potential and density wake behind a finite-sized object in a magnetized collisionless plasma flow is studied with self-consistent numerical simulations. With increasing magnetization of the plasma, the standard picture of ion focusing in the wake for plasmas with large electron to ion temperature ratios becomes invalid. A strong magnetic field parallel to the flow direction leads to a chain of ion depletions in the wake and enhanced ion density at their envelopes. This is due to a novel mechanism of a dynamic ion shadow, which is not the geometrical shadow of the finite-sized object. It corresponds to a change in topology of the wake potential. Complex ion trajectories resulting from electrostatic collisions with the object can lead to significant variations in electrical charging of other objects in the wake.

## 1. Introduction

Interactions of plasmas with finite-sized objects, such as dust particles and probes in laboratory plasmas or spacecrafts in the magnetosphere, are fundamental problems in the physics of plasmas [1–5]. The electric charge of the object determines the plasma density and potential profiles in its vicinity. For stationary conditions and isolated objects at floating potentials, when the net current to the surface vanishes, disturbances of the plasma will extend up to several Debye lengths [5]. The plasma flow with respect to the object gives rise to much further extending wakes in the plasma potential and density distributions, due to both surface absorption and electrostatic scattering of plasma particles at the object [6–8].

Wake effects have notable implications on the probe measurements in laboratory experiments [1], interpretation of data from spacecrafts [2], and charging and dynamics of systems comprising two or more dust particles exposed to the plasma flow, such as in complex (dusty) plasmas [5, 6]. There, accumulation of ions in the wake can lead to attractive, non-reciprocal forces, which lead to flow-aligned pairing, as observed in laboratory experiments and numerical simulations [9–16]. Ion focusing by the upstream object can also lead to a considerable reduction of the negative charge on downstream objects [15, 17].

Charging of (an) isolated object (s) in flowing *unmagnetized* plasmas has been a subject of extensive studies [6]. For large electron to ion temperature ratios, ions can be focused into the wake due to electrostatic scattering (deflection of ions) by a negatively charged object. This kinetic effect has been confirmed by both particle-in-cell (PIC) and molecular dynamics simulations [17–21]. The enhancement in ion density gives rise to a positive trailing peak in the potential distribution. The resulting oscillatory potentials in the wake correspond well to results obtained with the linear response (LR) theory [8] and can explain interactions between dust particle pairs in plasmas where collisions are negligible [17, 22]. Analogous studies contribute to the interpretation of data from spacecrafts in various plasma environments [2, 7, 23, 24].

Most previous theoretical studies have considered the wake formation in unmagnetized plasmas. However, in the view of recent dusty plasma experiments with external magnetic fields [25–27], and also in the general context of object–plasma interactions, it is of high urgency to understand the microphysics of wake formation in

© 2018 The Author(s). Published by IOP Publishing Ltd on behalf of Deutsche Physikalische Gesellschaft

magnetized plasmas. A few such attempts have been done recently with PIC simulations for $\vec{E} \times \vec{B}$ drifting plasmas, where $\vec{E}$ and $\vec{B}$ are, respectively, the electric and magnetic field [28, 29], as well as with the LR approach for a magnetic field aligned with the flow direction [30–34]. The latter configuration is relevant for recent experiments with dust particle pairs in magnetic fields [25]. With the LR approach, it has been demonstrated [32, 33] that with increasing magnetization, there is a change in topology of the wake potential: extrema in the wake become smaller and more frequent to eventually disappear at large values of the dynamic magnetization parameter $\beta_i = \omega_{ci}/\omega_{pi}$, where $\omega_{ci}$ is the ion cyclotron frequency and $\omega_{pi}$ is the ion plasma frequency. LR calculations provide only the wake potential distribution for a given charge/potential of a point-like object, and thus do not account for the self-consistent object charging and wake formation.

For finite-sized objects, one should also consider the geometrical magnetization parameter $\gamma_\alpha = r_p/r_{\mathrm{L}\alpha}$ for plasma species $\alpha$, which is the ratio of a characteristic radius of the object $r_p$ and the gyroradius of species $\alpha$, $r_{L\alpha}$. For $\gamma_\alpha > 1$ species $\alpha$ become magnetized from the point of view of the object. Under such conditions, the charging becomes increasingly anisotropic, and static magnetic shadowing, characterized by geometrical plasma depletion in the wake due to plasma absorption at the object, gets pronounced. This is in addition to dynamic ion shadowing which is related to strong scattering of plasma particles at the object for large $\beta_i$ as it is demonstrated in this paper.

To understand the wake formation and wake effects in magnetized plasmas on a kinetic level, also including charging of objects located in the wake, it is crucial to consider plasma particle trajectories in self-consistent force fields. In this work, we address the kinetics of plasma particles in magnetized collisionless plasma flows with full PIC simulations.

Our main objective is to explore the differences between unmagnetized and magnetized wakes and discuss the findings with respect to LR theory. A further goal is to analyze the fundamental mechanisms that underly new nonlinear phenomena in magnetized wakes. More detailed comparisons with experiments will be left to future investigations.

## 2. PIC simulations

We employ the DiP3D code, which advances trajectories of electrons and ions in self-consistent force fields in a three-dimensional Cartesian coordinate system. The details of the implementation are given in previous works [17, 35], and here we provide only the system parameters used for this study.

We simulate the plasma with a background density of $n_{i,0} = 10^{13}$ m$^{-3}$ and an electron temperature of $T_e = 3$ eV. The electron to ion temperature ratio is $T_e/T_i = 100$, which is typical for laboratory experiments of complex plasmas. The electron Debye length is set to $\lambda_{\mathrm{De}} = 4.03 \times 10^{-3}$m , and a three-dimensional simulation box extends 0.05 m in each direction. We consider an open system with supersonic plasma flows of $v_d = 1.2c_s$ and $v_d = 2.4c_s$, with the sound speed given by $c_s = \sqrt{(kT_e + 5kT_i/3)/m_i}$ , where $k$ is the Boltzmann constant. This gives Mach numbers $M = v_d/c_s$ of $M = 1.2$ and $M = 2.4$. The ion to electron mass ratio is set to $m_i/m_e = 900$, which is close to the conditions in a hydrogen plasma, but allows for a reasonable computing time. Thus, the choice of parameters is a compromise between the numerical constraints and experimental conditions [15]. The magnetic field is aligned with the flow. By varying $\|\vec{B}\|$, we consider different dynamic magnetizations of plasma, $\beta_i \in (0,\ 6.6)$, which correspond to magnetic fields of approximately $\|\vec{B}\| \in (0,\ 200)$mT for our choice of parameters. Note, that in case of argon plasmas, which are often used in laboratory experiments, this range represents an equivalent magnetic field, which is 82 times larger and reaches a maximum of $B = 1.8$ T. In this way, the accessible range with superconducting magnets, $B < 5$ T, is partially covered by the present simulations. In addition, in order to relate our results to recent studies with the LR approach [33], we run simulations for $M = 1.0$ and $\beta_i = 1.5$. An additional run at $m_i/m_e = 450$ was made to study the influence of an enhanced ion thermal motion.

A spherical conducting object of radius $r_p \sim 0.1\lambda_{\mathrm{De}}$ , where $\lambda_{\mathrm{De}} = \sqrt{\epsilon_0 kT_e/n_e e^2}$ is the electron Debye length, is placed far away from the boundaries. Here, $\epsilon_0$, $e$, $n_e$ are, respectively, the electric permittivity of vacuum, electron charge, and the electron number density. Since the DiP3D code is optimized for finite-sized objects consisting of dielectric and conducting materials, the chosen object size is a necessary trade-off. The object is charged self-consistently by electron and ion collection currents during the simulation. Upon hitting the object surface, the plasma particles are removed from the simulation and contribute to the total charge on the object. The results presented in the following correspond to steady-state conditions for object charging, which are usually reached after several ion plasma periods $2\pi/\omega_{pi}$ .

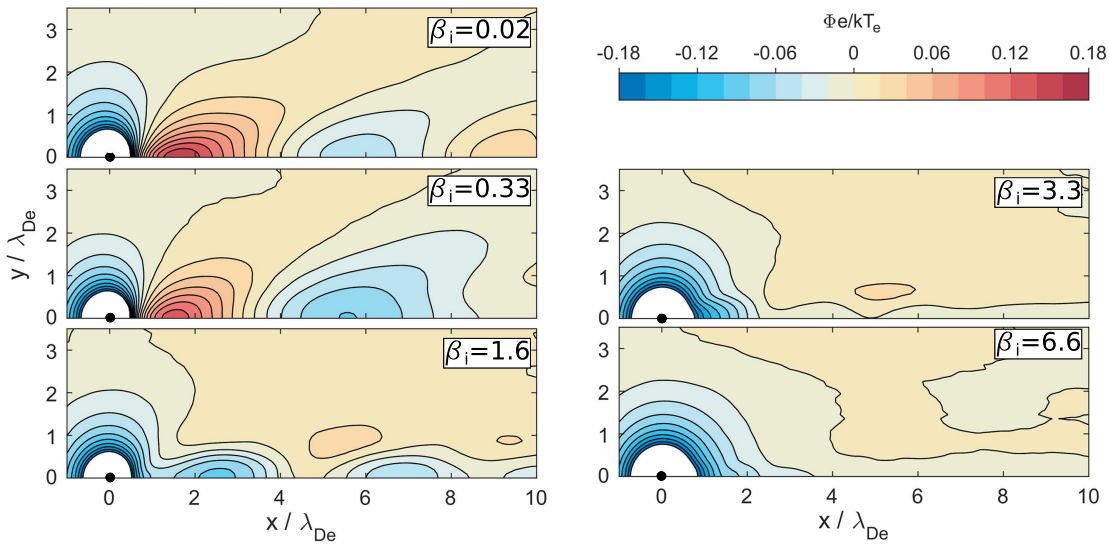


**Figure 1.** Potential distributions in $x$–$y$ planes through the center of the object for different dynamic magnetizations $\beta_i = (0.02, 0.33, 1.6, 3.3, 6.6)$ for $M = 1.2$. The plasma flow and magnetic field are in the positive $x$ direction. To emphasize wake features, only the shallow potential variations are colored. Due to cylindrical symmetry around the $x$-axis, results for $y < 0$ are not shown.

## 3. Results

Figure 1 presents slices of the electric potential distribution in the $x$–$y$ plane for different dynamic magnetizations $\beta_i$. For very low $\beta_i$, the potential variation in the wake resembles the case of unmagnetized plasma flow [15]. With increasing $\beta_i$, the trailing peak becomes smaller and moves upstream. At the same time the minima that follow become more pronounced. For $\beta_i > 1$, the topology of the wake changes significantly: the trailing peak eventually disappears behind the object and subsequent minima form a chain-like structure. The potential distribution is mostly positive in the wake, and this feature is pronounced away from the symmetry axis. At higher $\beta_i$, the oscillatory pattern gets less pronounced to finally disappear. Here, the dominant structure in the wake is the extended positive potential with a narrow negative potential line along the flow direction centered at the object.

With respect to general tendencies, the results from our PIC simulations agree with recent results obtained with the LR approach by Joost *et al* [33]. In both PIC and LR approaches, with increasing $\beta_i$, the potential maxima move upstream and get more frequent, and finally a positive potential distribution appears in the wake off the symmetry axis. However, for $\beta_i > 1$ there is a significant difference between the results obtained with the two approaches along the symmetry axis in the wake. In PIC simulations, ion shadowing results in a negative potential along the symmetry axis in the wake with superimposed oscillations, and this negative potential is not present in the LR approach.

This is emphasized in figure 2, which shows the potential distribution in the $x$–$y$ plane from PIC simulations, and the potential cut in the $x$ direction through the object for two ion to electron mass ratios for $\beta_i = 1.5$ and $M = 1$. Lower mass ratio results in larger thermal velocity of ions, when other parameters remain unchanged, and hence weaker focusing and smaller oscillations in the wake potential. More heavy and hence more realistic ions, give significant oscillations and well pronounced potential minima in the wake. There is no agreement in the position of maxima along the symmetry line in the two cases, and no clear scaling with respect to the mass ratios or their square root. We note that in both cases the ion focus is at the same distance from the object although it is stronger for heavier ions, and that the object's potential is only marginally different in these two cases, $\Phi \approx -1.67\, kT_e/e$.

The results from the LR approach taken along the symmetry axis downstream of the object [33], shown for comparison in figure 2(b), do not agree with PIC results. However, the overall wake patterns at larger scales and far from the symmetry axis for the two methods approach one another. This suggests that, to a first-order approximation, nonlinear effects can be disregarded in the studies of wake formation in weakly magnetized plasmas at large scales. However, comparison of results from these two approaches in figure 2(b) reveals that the wake pattern directly downstream of the object can be substantially different. LR addresses a point-like disturbance and does not capture the effects of static magnetic shadowing behind finite-sized objects at large $\gamma_\alpha$. Since LR does not provide information on the plasma particle kinetics, it does not give insight into dynamic shadowing neither. Magnetic shadowing effects can have significant implications on the charge distribution in

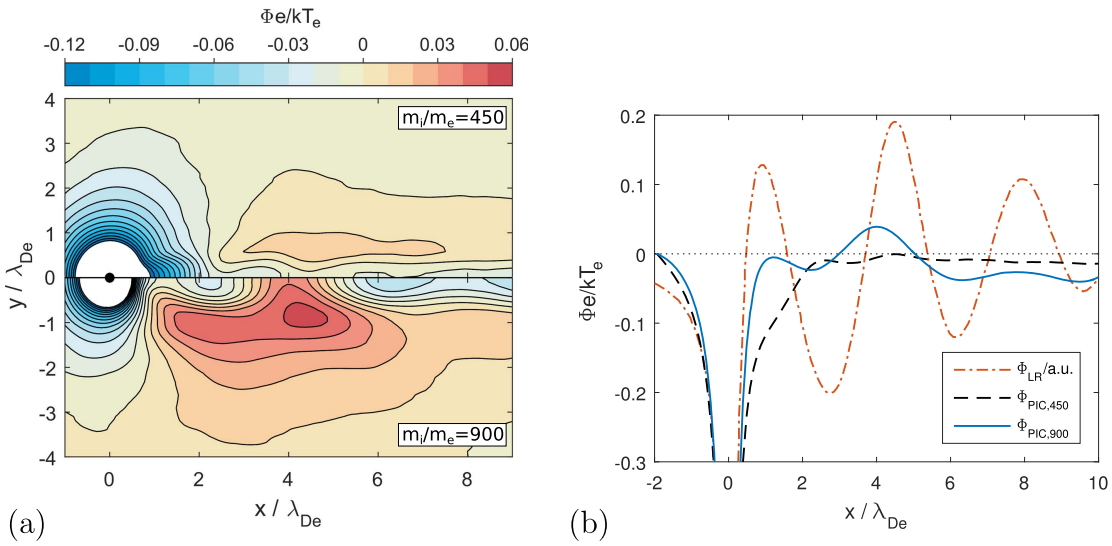


**Figure 2.** Potential distributions in $x$–$y$ planes for $\beta_i \approx 1.5$ and $M = 1$ for (a) $m_i/m_e = 900$ and $m_i/m_e = 450$, as well as (b) along the $x$-axis through the center of the object. For comparison, the result from LR calculations (figure 6 in [33]) at the same $\beta_i$ and $M$ are also depicted in (b).

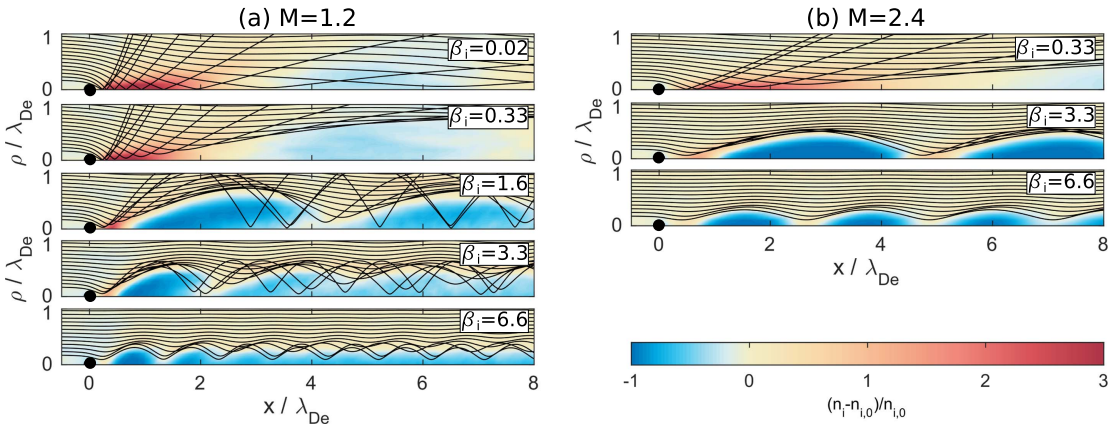


**Figure 3.** Test particle trajectories plotted on-top of normalized ion density distributions in the $x$–$\rho$ plane (cylindrical symmetry) for $M = 1.2$ (a) and $M = 2.4$ (b) for different magnetizations $\beta_i$; $m_i/m_e = 900$. Only trajectories of ions entering the wake are shown.

the wake, and also charging of objects in such wakes. Fortunately, microphysics leading to the change in wake topology with increasing magnetization of the plasma can be studied in detail with PIC simulations.

Ion density distributions from our PIC simulations for different $\beta_i$ are shown in figure 3 for $m_i/m_e = 900$ and two velocities: $M = 1.2$ and $M = 2.4$, together with the corresponding test particle trajectories for cold ions that enter the wake. The cold ion approximation is justified for supersonic flows, where for our choice of parameters, the thermal velocity of ions is one order of magnitude smaller than the drift velocity. The ion density distributions reveal that with increasing $\beta_i$ , ion focusing gets weaker and moves closer towards the object. Finally, for large $\beta_i$ the topology of the focusing region changes. The ions are still scattered into the wake, but they form a wing-like structure at an angle to the drift velocity. This angle is related to the flow velocity, being smaller for faster flows. In the flow direction, the v-shaped wing-like structure is directly followed by a localized depletion in the ion density, the dynamic ion shadows. Dynamic ion shadowing gives almost ion-free areas that are surrounded by enhanced density with strong density gradients in the envelope region. This pattern is repetitive and results in the chain of ion depletions.

For magnetized plasmas $\beta_i > 1$, ions get scattered and accelerated in the vicinity of the object, and continue along helical orbits in the wake. We observe both an overall depletion in the ion density in the wake along the symmetry axis, as well as periodic enhancements in the ion density related to the helical motion of ions. For a given $\beta_i$, the frequency of enhancements in the wake increases (i.e., regions with depleted ion density get larger) with the flow velocity $v_d$ , while for a given $v_d$, the frequency decreases with increasing $\beta_i$ .

The chains of ion depletions and sharp density gradients at their envelopes can also be addressed by studying particle trajectories with an effective potential of the obstacle, where a radially symmetric Coulomb field can be taken as an approximation. Ion scattering happens at time-scales much shorter than the gyroperiod and can be considered as a classical Rutherford scattering. Thus, scattering events in magnetized flows can be decomposed into outer trajectory parts, where the particles follow the Lorentz force, and a nearly unmagnetized scattering event within a 'collision sphere', the radius of which is determined by the ion impact parameter. The scattering results in a dynamic shadow characterized by complex distributions of density and potential in the wake.

## 4. Discussion and conclusions

In addition to the flow velocity $v_d$, several parameters can influence the formation of a magnetized wake. The dynamic magnetization $\beta_i = \omega_{ci}/\omega_{pi}$ reflects the anisotropy of plasma. For $\beta_i > 1$ the ion Larmor radius becomes smaller than the ion Debye length, $r_{Li} < \lambda_{Di}$, and ion dynamics will be dominated by the magnetic field. In agreement with the LR approach, we observe an overall change in wake topology for $\beta_i > 1$. Furthermore, the efficiency of collisions $c_{\rm ef} = \omega_{ci}\,\tau_{\rm col}$, where $\tau_{\rm col}$ is the characteristic collision time between the ion and the object, can be related to the size of ion density shadows. Larger $\|\overrightarrow{B}\|$ (i.e., shorter gyroperiod) reduces the time interval when ions are subject to scattering, and gives smaller and more frequent density depletions. More efficient scattering for small $\|\overrightarrow{B}\|$ allows for larger acceleration of ions in both perpendicular and parallel directions, and hence larger helices and extent of depletions. The collision time depends on both $r_{Li}$ and the strength of the electric field in the vicinity of the object. The scattering process and, hence, the phenomenon of dynamic shadow formation are nonlinear, and are not captured with the LR approach.

Another parameter is the geometrical magnetization $\gamma_\alpha$, which relates to a static shadow in the wake. For the flow velocities considered in our work, this effect is most pronounced for ions, and electrons can be assumed stationary with respect to the object. For large magnetic fields, $\gamma_i > 1$ and the static ion shadow contributes to a negative potential along the symmetry line in the wake in the closest vicinity of the object. Note that this static ion shadowing appears in addition to dynamic ion shadowing due to ion scattering at the object in strongly magnetized plasma flows.

Dynamic shadowing resulting in chains of depletions and enhancements in the ion density not only explains the potential variations in the wake, but also has implications on the charging of other objects, such as dust particles, in magnetized collisionless plasma flows. The structure of the wake implies that there may exist either attractive or repulsive interparticle forces depending on the location of the downstream particle. Non-trivial charge distributions on downstream dust particles in magnetized plasmas will affect dust interactions and structuring of dust clusters [25, 26]. This knowledge on charging and wake structure in strong magnetic fields will contribute to our understanding of dust dynamics in magnetized plasmas [27].

High dynamic magnetizations $\beta_i$ can be encountered in many laboratory experiments, such as in Q-machines [36, 37] or rf discharges inside superconducting magnets [25, 26], and in such cases the diagnostics should take the dynamic shadows into account. We note that in our study, we consider large electron to ion temperature ratios. For smaller temperature ratios, the shadowing may get reduced due to larger ion thermal velocity. On the other hand the shadowing will get enhanced for larger ion to electron mass ratios.

The present study considers collisionless plasma flows. Such plasma conditions are relevant for space plasmas or some experiments. Collisions with neutrals can significantly influence the plasma particle dynamics, especially in the presence of external magnetic fields. In a limiting case, they can lead to effective demagnetization of ions. Thus, the effect of collisions on the formation and persistence of wake in magnetized plasmas should be a subject of further investigations.

To summarize, with kinetic PIC simulations we have shown that for strongly magnetized collisionless plasmas, the nonlinear dynamic shadowing in the wake results in periodic ion-free regions with envelopes of elevated ion density. This new feature has implications on charging characteristics, dust interactions and dynamics, and plasma diagnostics in strongly magnetized wakes.

## Acknowledgments

Work at the University of Oslo (UiO) was supported by Research Council of Norway, project number 240000. It is also a part of 4DSpace Strategic Research Initiative at UiO. Part of the investigations at Kiel University had been financially supported by DFG within the Transregional Collaborative Research Centre TR-24, project A2.

## ORCID iDs

W J Miloch https://orcid.org/0000-0002-5202-750X
H Jung https://orcid.org/0000-0003-0004-1518
D Darian https://orcid.org/0000-0002-8550-3525
F Greiner https://orcid.org/0000-0002-4828-3770

## References

[1] Rubinstein J and Laframboise J G 1982 Theory of a spherical probe in a collisionless magnetoplasma *Phys. Fluids* **25** 1174–82
[2] Berthelier J J and Roussel J F 2004 A study of the electrical charging of the rosetta orbiter: II. Experimental tests in a laboratory plasma *J. Geophys. Res.* **109** A01105
[3] Garrett H B 1981 The charging of spacecraft structures *Rev. Geophys.* **19** 577
[4] Whipple E C 1981 Potentials of surfaces in space *Rep. Prog. Phys.* **44** 1197
[5] Shukla P K and Mamun A A 2002 *Introduction to Dusty Plasmas* (Bristol: Institute of Physics Publishing)
[6] Fortov V E, Ivlev A V, Khrapak S A, Khrapak A G and Morfill G E 2005 Complex (dusty) plasmas: current status, open issues, perspectives *Phys. Rep.* **421** 1–103
[7] Marchand R *et al* 2014 Cross-comparison of spacecraft-environment interaction model predictions applied to solar probe plus near perihelion *Phys. Plasmas* **21** 062901
[8] Ludwig P, Miloch W J, Kählert H and Bonitz M 2012 On the wake structure in streaming complex plasmas *New J. Phys.* **14** 053016
[9] Trottenberg T, Melzer A and Piel A 1995 Measurement of the electric charge on particulates forming Coulomb crystals in the sheath of a radiofrequency plasma *Plasma Sources Sci. Technol.* **4** 450
[10] Hayashi Y and Tachibana K 1996 Coulomb crystal formation from growing particles in a plasma and the analysis *J. Vac. Sci. Technol.* A **14** 506–10
[11] Melzer A, Schweigert V A, Schweigert I V, Homann A, Peters S and Piel A 1996 Structure and stability of the plasma crystal *Phys. Rev.* E **54** R46
[12] Schweigert V A, Schweigert I V, Melzer A, Homann A and Piel A 1996 Alignment and instability of dust crystals in plasmas *Phys. Rev.* E **54** 4155–66
[13] Melzer A, Schweigert V A and Piel A 1999 Transition from attractive to repulsive forces between dust molecules in a plasma sheath *Phys. Rev. Lett.* **83** 3194–7
[14] Takahashi K, Oishi T, Shimomai K-I, Hayashi Y and Nishino S 1998 Analyses of attractive forces between particles in Coulomb crystal of dusty plasmas by optical manipulations *Phys. Rev.* E **58** 7805–11
[15] Miloch W J, Kroll M and Block D 2010 Charging and dynamics of a dust grain in the wakefield of other grain *Phys. Plasmas* **17** 103703
[16] Piel A 2017 Molecular dynamics simulation of ion flows around microparticles *Phys. Plasmas* **24** 033712
[17] Miloch W J and Block D 2012 Dust grain charging in a wake of other grains *Phys. Plasmas* **19** 123703
[18] Miloch W J, Trulsen J and Pécseli H L 2008 Numerical studies of ion focusing behind macroscopic obstacles in a supersonic plasma flow *Phys. Rev.* E **77** 056408
[19] Hutchinson I H 2005 Ion collection by a sphere in a flowing plasma: III. Floating potential and drag force *Plasma Phys. Control. Fusion* **47** 71–87
[20] Maiorov S A, Vladimirov S V and Cramer N F 2000 Plasma kinetics around a dust grain in an ion flow *Phys. Rev.* E **63** 017401
[21] Lapenta G 1999 Simulation of charging and shielding of dust particles in drifting plasmas *Phys. Plasmas* **6** 1442–7
[22] Hutchinson I H 2011 Forces on a small grain in the nonlinear plasma wake of another *Phys. Rev. Lett.* **107** 095001
[23] Yaroshenko V V, Miloch W J, Vladimirov S, Thomas H M and Morfill G E 2011 Modeling of Cassini's charging at Saturn orbit insertion flyby *J. Geophys. Res.* **116** A12218
[24] Marchand R and Resendiz Lira P A 2017 Kinetic simulation of spacecraft—environment interaction *IEEE Trans. Plasma Sci.* **45** 535–54
[25] Carstensen J, Greiner F and Piel A 2012 Ion-wake-mediated particle interaction in a magnetized-plasma flow *Phys. Rev. Lett.* **109** 135001
[26] Thomas E Jr, Merlino R L and Rosenberg M 2012 Magnetized dusty plasmas: the next frontier for complex plasma research *Plasma Phys. Control. Fusion* **54** 124034
[27] Thomas E Jr, Konopka U, Merlino R L and Rosenberg M 2016 Initial measurements of two- and three-dimensional ordering, waves, and plasma filamentation in the magnetized dusty plasma experiment *Phys. Plasmas* **23** 055701
[28] Patacchini L and Hutchinson I 2011 Spherical conducting probes in finite Debye length plasmas and E × B fields *Plasma Phys. Control. Fusion* **53** 025005
[29] Darian D, Marholm S, Paulsson J J P, Miyake Y, Usui H, Mortensen M and Miloch W J 2017 Numerical simulations of a sounding rocket in ionospheric plasma: effects of magnetic field on the wake formation and rocket potential *J. Geophys. Res.* **122** 9603–21
[30] Nitta H, Nambu M, Salimullah M and Shukla P K 2003 Dynamical potential in a magnetized plasma *Phys. Lett.* A **308** 454
[31] Bhattacharjee S and Das N 2012 Effect of wake potential on Coulomb crystallization in the presence of magnetic field *Phys. Plasmas* **19** 103707
[32] Bezbaruah P and Das N 2017 Wake potential in 2-d magnetized complex plasma *Eur. Phys. J.* D **71** 114
[33] Joost J-P, Ludwig P, Kählert H, Arran C and Bonitz M 2015 Screened Coulomb potential in a flowing magnetized plasma *Plasma Phys. Control. Fusion* **57** 025004
[34] Kählert H, Joost J P, Ludwig P and Bonitz M 2016 Streaming complex plasmas: ion susceptibility for a partially ionized plasma in parallel electric and magnetic fields *Contrib. Plasma Phys.* **56** 204–14
[35] Miloch W J 2015 Simulations of several finite-sized objects in plasma *Proc. Comput. Sci.* **51** 1282–91
[36] Koepke M E, Zintl M W, Teodorescu C, Reynolds E W, Wang G and Good T N 2002 Inhomogeneous magnetic-field-aligned ion flow measured in a Q machine *Phys. Plasmas* **9** 3225–35
[37] Schmitt J P M 1971 Wake behind an obstacle in a single-ended Q-machine and its use as a diagnostic of the ion distribution function *Proc. 3rd Int. Conf. on Quiescent Plasmas (Elsinore , 20–24 September 1971)* pp 185–93